Astron. Astrophys. 173, 167–179 (1987)

ASTRONOMY AND ASTROPHYSICS

Diagnostics of solar magnetic fluxtubes with the infrared line Fe I λ 15648.54 Å

J.O. Stenflo[1,★], S.K. Solanki[1,★], and J.W. Harvey[2]

[1] Institute of Astronomy, ETH-Zentrum, CH-8092 Zürich, Switzerland
[2] National Solar Observatory, National Optical Astronomy Observatories★★, P.O. Box 26732, Tucson, AZ 85726, USA

Received August 20, accepted September 1, 1986

Summary. The center-to-limb variation of the Stokes *I*, *V*, and *Q* profiles of the infrared line Fe I λ 15648.54 Å has been observed with a Fourier transform spectrometer to explore the new possibilities offered for the diagnostics of the spatially unresolved magnetic fluxtubes on the sun when lines with complete Zeeman splitting are used. As this infrared line is located where the continuum opacity has a minimum, deeper atmospheric layers can be diagnosed than in any other spectral range.

The observed Zeeman splitting as a function of center-to-limb distance provides direct information on the height variation of the field strength and fluxtube radius. Comparison is made with the line-ratio method, which has to be used at visible wavelengths, where the splitting is incomplete. The field strength obtained from the 15648.54 Å line is about 20% larger than that found from the 5250.22 Å line, which is consistent with the observed center-to-limb variation of the field strength and the lower height of formation of the 15648.54 Å line. The large splitting of the infrared line further makes the Zeeman broadening of each σ component directly visible, which may be used to derive the lateral *distribution* of the field strengths inside the spatially unresolved fluxtubes.

The Stokes *V* asymmetries observed in the infrared line are small or even of opposite sign as compared with the corresponding asymmetries observed at visible wavelengths. This suggests that the time-averaged height gradient of the Doppler velocities inside the fluxtubes becomes small and may change its sign when moving down to the bottom of the fluxtube photosphere.

Key words: solar magnetic fields – fluxtubes – Stokes parameters – line profiles – infrared radiation

1. Introduction

When the strong-field (kG) nature of photospheric solar magnetic fields was revealed in the early 1970s, two observational approaches played a leading role: (1) The line-ratio technique, with which the Zeeman-effect polarization is recorded simultaneously in two carefully selected spectral lines. (2) Measurements of the Zeeman splitting of the infrared line Fe I λ 15648.54 Å.

The line-ratio technique was exploited fairly systematically, to determine both the field strength and temperature structure of the spatially unresolved magnetic fluxtubes, revealing that more than 90% of the detectable flux is in strong-field form and that the field strengths are practically the same in the quiet network as in strong active-region plages (Stenflo, 1973, 1975, 1976). The Zeeman splitting of the infrared line gave field strengths slightly larger than the line-ratio technique (Harvey and Hall, 1975; Harvey, 1977), independently demonstrating again the extreme intermittency of the solar magnetic field. This potentially very powerful method was however not exploited more extensively because of inadequate spectrometers and infrared detectors.

With the availability of the FTS (Fourier transform spectrometer) Stokes polarimeter of the McMath telescope at the National Solar Observatory (Brault, 1978), a more general and unified approach to the problem of fluxtube diagnostics has become possible. As the FTS polarimeter can provide spectrally completely resolved Stokes line profiles with high signal-to-noise ratio and simultaneous coverage of large spectral ranges, we are not as in the past limited to comparing the polarization in certain spectral windows and pairs of lines, but can use the full profile information in hundreds of simultaneously recorded spectral lines.

To be able to fully exploit the enormous potential of the FTS polarimeter data we first need to, step by step, explore the diagnostic contents of the Stokes spectra, develop the appropriate diagnostic tools, and deepen our understanding of the fluxtube physics involved. Accordingly our first step was an exploratory analysis of a few selected lines in the Stokes *I* and *V* FTS spectra recorded near disk center in April 1979 (Stenflo et al., 1984; Stenflo and Harvey, 1985). This was followed by the application of a statistical approach to the same data, analysing a set of 400 Fe I and 50 Fe II simultaneously recorded, unblended Stokes profiles (Solanki and Stenflo, 1984, 1985). The next step was to investigate the center-to-limb variation of the Stokes profiles and to include the linear polarization (Stokes *Q*) in the analysis. Thus, based on FTS observations of May 1984, the diagnostic contents of the center-to-limb variations of the Stokes *I*, *V*, and *Q* profiles was explored by analysing in detail the behaviour of the lines within the range 5246–5252 Å (Stenflo et al., 1986).

In the present paper we will use the FTS recordings of May 1984 to explore the center-to-limb variation of the Stokes *I*, *V*, and *Q* profiles of the infrared line Fe I λ 15648.54 Å that was used by Harvey and Hall in the 1970s. The aim is to explore the

Send offprint requests to: J.O. Stenflo
★ Visiting astronomer, National Solar Observatory★★
★★ Operated by the Association of Universities for Research in Astronomy, Inc., under contract with the National Science Foundation

potential of this line for fluxtube diagnostics, and to clarify how the information it provides relates to and complements the diagnostic information obtained by the line-ratio technique, or by other methods in the visible part of the spectrum. Such a "unification" of the various previous methods has now become possible because of the complete spectral information provided by the FTS.

There are two major advantages of this infrared portion of the spectrum for fluxtube diagnostics. The main advantage is that the Zeeman splitting increases with wavelength. In the infrared we can find lines, like the one that will be explored in the present paper, which are completely Zeeman split in the fluxtubes. In the visible no such line can be found. Another advantage is that the minimum of the continuum opacity occurs around $\lambda \approx 1.65\,\mu$m. At these wavelengths we can therefore penetrate to the largest depths in the atmosphere.

In Fig. 1 we have plotted a 10 Å portion (15646–15656 Å) of FTS Stokes I, V, and Q recordings made on May 7, 1984, in a sunspot at μ (cosine of the heliocentric angle) = 0.47, and in a plage at $\mu = 0.61$. Of the two spectral lines seen it is the left one that is to be analysed in the present paper. This Fe I line at 15648.54 Å is produced by the transition $5s\,^7D_1$–$5p\,^7D_1$ (Litzén, 1976), the excitation potential of the lower level being 5.43 eV. It is a normal Zeeman triplet with a large Landé factor of 3.00. The spectral line to the right of it, at 15652.87 Å, is also an Fe I line, due to the transition $^7D_1^\circ$–$^3D_1$ (Goldberg et al., 1949). It has an effective Landé factor of 1.865 and an excitation potential of its lower level of 2.47 eV.

The sunspot recording of Stokes I demonstrates the large splitting of the 15648.54 Å line, the splitting of the 15652.87 Å line being less complete. From the Stokes I and V recordings we notice that there is a blend line in the red σ component of the 15648.54 Å line in the sunspot, which does not seem to be present in the plage (as judged from the Stokes V recording there). This blend is probably due to a molecular line (OH?) that has significant strength only in cool sunspot umbrae. The plage recording also has widely separated σ components, but they are difficult to discern in the Stokes I spectrum, which is dominated by the narrow, unpolarized, and non-split central component. The σ components are located in the far line wings and are very weak, due to the small magnetic filling factor (fractional area covered by magnetic fields) in the plage. As these distant portions of the line

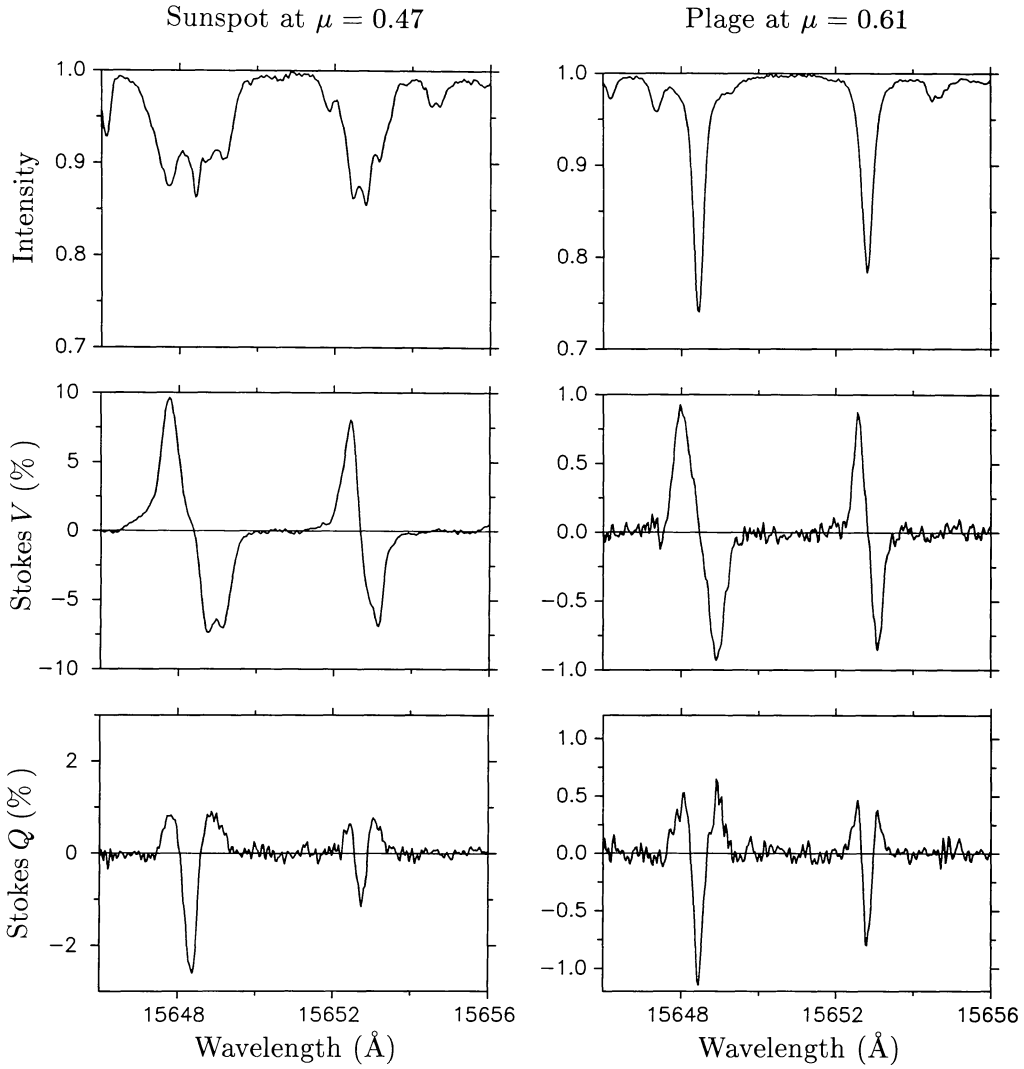

Fig. 1. Stokes I, V, and Q spectra over the range 15646–15656 Å, recorded with the NSO McMath FTS polarimeter on May 7, 1984, in a sunspot at $\mu = 0.47$ (left diagrams) and a plage at $\mu = 0.61$ (right diagrams). V and Q are given in units of the intensity of the adjacent continuous spectrum

wings are very susceptible to blends, the unpolarized I spectrum is not well suited for determinations of the Zeeman splitting, but one needs the polarization information.

2. Relation between magnetic-field diagnostics in the visible and in the infrared

The main advantage of using an infrared line like Fe I λ 15648.54 Å is the large Zeeman splitting as compared with the line width at these longer wavelengths. Whereas the Zeeman splitting increases with the square of the wavelength, the widths of the spectral lines are in a first approximation proportional to the wavelength itself. Thus, at 15000 Å the ratio between Zeeman splitting and line width has increased by typically a factor of three as compared with the spectrum around 5000 Å.

In the visible, the widely used line Fe I λ 5250.22 Å has one of the largest Zeeman splittings. Like the 15648.54 Å line it is a normal Zeeman triplet with a Landé factor of 3.00. Its most important use has been for the line-ratio technique, together with the neighbouring Fe I line of the same multiplet, at 5247.06 Å with an effective Landé factor of 2.00. Accordingly we will use this line pair, and in particular the 5250.22 Å line, as a reference when evaluating the diagnostic possibilities with the 15648.54 Å line.

The amount of circular polarization (amplitude of Stokes V) is in a first approximation proportional to the magnetic flux (along the line of sight) inside the spatial resolution element, but by itself it does *not* provide any information on the magnetic field strength. The field-strength information is contained in the *shape* of the Stokes V profile. To understand this problem it is useful to distinguish between essentially three regimes for the Zeeman-split lines in the solar spectrum: (1) The weak-field regime (splitting insignificant in comparison with the line width). (2) Partial splitting. (3) Complete splitting. As we shall see below, the great majority of lines in the visible spectrum belongs to category (1), the 5250.22 Å line to category (2), and the 15648.54 Å line to category (3) (except at the extreme limb, where it seems to move down to the lower categories). Next we will see the explicit connection between these categories, to understand how the various types of diagnostic methods relate to each other.

For a normal Zeeman triplet in a constant magnetic field parallel to the line of sight we can express Stokes V in terms of Stokes I as the difference between the Zeeman-shifted σ components of the line:

$$V = \tfrac{1}{2}[I(\lambda + \Delta\lambda_H) - I(\lambda - \Delta\lambda_H)] \tag{1}$$

(Stenflo, 1985). If the Zeeman splitting is not large as compared with the line width a Taylor expansion of (1) is useful:

$$V = \Delta\lambda_H \left[\frac{\partial I}{\partial \lambda} + \tfrac{1}{6}(\Delta\lambda_H)^2 \frac{\partial^3 I}{\partial \lambda^3} + \cdots \right]. \tag{2}$$

For small splittings, the higher-order terms in the expansion become insignificant, and only the first term needs to be retained. This is what we mean by the "weak-field regime" mentioned above. When the magnetic flux does not cover the spatial resolution element but only a small fraction thereof (filling factor α is small), which is practically always the case, we must keep in mind that V scales with α. Thus for weak fields V is proportional to the product αB, i.e., the magnetic flux, but α and the field strength B cannot be separately determined. It is the higher-order terms in the expansion, i.e., the non-linearities in the relation between V and B, which allow a determination of B alone. The non-linear effects change the *shape* of the V profile.

In the weak-field regime the shape of the V profile is given by $\partial I/\partial\lambda$, and the wavelength separation between the V profile peaks in the blue and red line wings simply equals the separation between the inflexion points in the Stokes I profile, and thus contains no information on the field strength B. For a completely split line, on the other hand, the separation between the V peaks equals the Zeeman splitting, which means that B can be obtained directly. For partial splitting B can also be evaluated, although its extraction is less direct as compared with the complete-splitting case. It was to avoid model dependence in this B evaluation for partially split lines that the line-ratio method was devised.

For a Gaussian Stokes I profile the distance from the line center to each inflexion point is $0.425\,\Delta\lambda_I$, where $\Delta\lambda_I$ is the total half width (full width at half maximum) of the profile. Let us normalize all wavelength differences in terms of this distance, i.e., introduce a dimensionless wavelength scale v, defined by

$$v = \Delta\lambda/(0.425\,\Delta\lambda_I), \tag{3}$$

where $\Delta\lambda$ is the wavelength distance from the line center. Let us also apply this scale to any non-Gaussian profile shapes. Then we can write (2) as

$$V = v_H \frac{\partial I}{\partial v} + \cdots, \tag{4}$$

where v_H is $\Delta\lambda_H$ normalized to the same scale as v. If we let v_D be the Doppler width of a Gaussian profile with the same total half width $\Delta\lambda_I$ as the spectral line considered, we can use v_D expressed in velocity units instead of $\Delta\lambda_I$ to represent the line width, as was done in Stenflo and Lindegren (1977) and Solanki and Stenflo (1984, 1985). Then, with our normalization,

$$v_H = 1.98 g\lambda B/v_D \tag{5}$$

if λ is expressed in μm, B in kG, and v_D in km s^{-1}. g is the Landé factor.

In a first approximation v_D, being expressed in velocity units, is wavelength independent. v_H thus scales in direct proportion to λ. As the expansion (4) is in terms of v_H, the non-linear effects (importance of higher-order terms in the expansion) are generally much more pronounced in the infrared. In the limit of large v_H we should reach the full splitting case. Next we will illustrate this transition from the weak-field to the complete splitting case.

To clarify this transition we will use model calculations with Voigt functions to represent the I profiles (σ components) in (1). It turns out that with our wavelength normalization, the results are insensitive to the actual shape of the line profile (here modelled via the Voigt damping parameter). We have calculated theoretical V profiles for a range of v_H values. From the theoretical profiles we can extract the same profile parameters that we have used (and will be using in the present paper) in the analysis of the observed profiles (cf. Stenflo et al., 1986), and plot them as a function of v_H. Thus Fig. 2 shows the V peak separation and the V amplitude as functions of $v_H = \Delta\lambda_H/(0.425\,\Delta\lambda_I)$.

In the left diagram of Fig. 2 we have plotted half the wavelength separation between the red and blue Stokes V peaks, $0.5(\lambda_{V_r} - \lambda_{V_b})$, normalized to the v scale, vs. v_H. $\lambda_{V_{r,b}}$ is defined as the center of gravity of the part of the V profile above the level

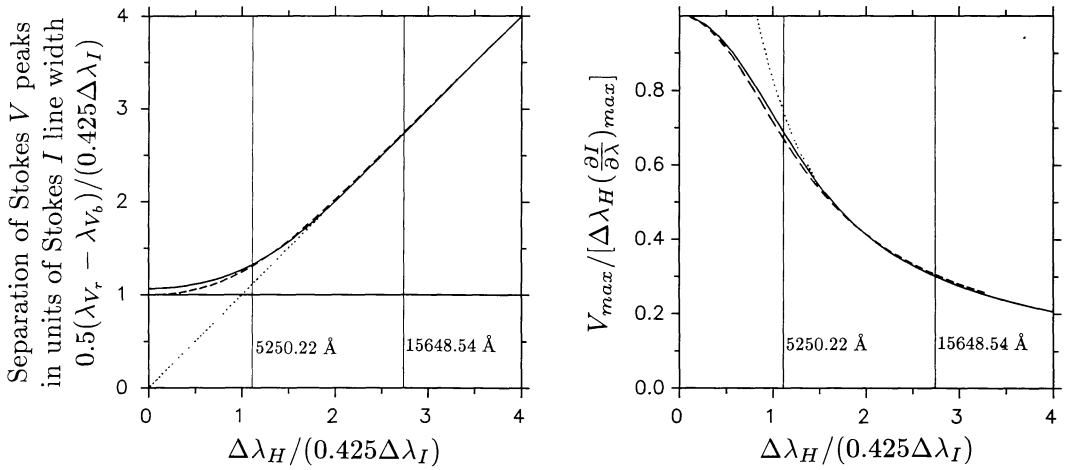

Fig. 2. Illustration of the transition from the weak-field to the strong-field (complete splitting) regime, using Voigt profiles for I in Eq. (1), with damping constants zero (solid curves) and 0.4 (dashed curves). The separation of the center of gravities of the upper halves of the red and blue Stokes V peaks (left diagram) and the V amplitude normalized to its value in the weak-field limit (right diagram) are plotted vs. the Zeeman splitting in units of the line width, as defined in the text ($\Delta\lambda_I$ is the total half width of Stokes I). The dotted curves represent the asymptotic strong-field limits, extrapolated to small values of the Zeeman splitting. The vertical lines indicate the location of the disk-center profiles of the 5250.22 and 15648.54 Å lines in the case of a 1 kG magnetic field

halfway between the zero line and the peak value. This definition provides a numerically more stable peak position of the observed profiles than the position of the very peak, due to noise in the data. The solid curve gives the results when Gaussian σ components are used, while the dashed curve is based on a Voigt profile with damping constant = 0.4 (in units of the Doppler width). The dotted curve is the 45° line.

The diagram clearly illustrates the transition between the weak and strong-field case. In the limit of small splittings v_H, the normalized peak separation is about unity (not exactly unity because of the center-of-gravity definition of $\lambda_{V_{r,b}}$), the separation between the Stokes I inflexion points, independent of v_H. In the limit of large splittings the curves coincide with the 45° line, i.e., the V peak separation is simply the splitting itself. The transition between these two regimes occurs in the range $0.5 \lesssim v_H \lesssim 1.5$.

With the two vertical lines in the diagram we have marked where the disk-center profiles of the two spectral lines at 5250.22 and 15648.54 Å belong, in the case of a field strength $B = 1$ kG. At disk center their observed line widths v_D are 2.81 and 3.39 km s^{-1}, respectively. Whereas the infrared line lies well within the completely split regime, the 5250.22 Å line is located in the middle of the intermediate-splitting, transition regime, where the deviation from the weak-field level is appreciable, but the 45° line has not yet been reached.

The corresponding v_H position of the 5247.06 Å line in the diagram is at $\frac{2}{3}$ times that of the 5250.22 Å line, since v_H scales with the Landé factor, and these two lines have the same line width. The 5247.06 line is substantially closer to the weak-field level than the 5250.22 line, so the ratio between them provides information about the magnitude of v_H and thus of B (the observed V peak separation in 5250.22 alone is not a reliable measure of the field strength, since $\Delta\lambda_I$ of the I profile that originates exclusively in the spatially unresolved fluxtubes is not observable). As the solid curve is somewhat flatter than the dashed curve, there will be a profile shape dependence of the results when this line ratio is used. This profile shape dependence is however insignificant in the case of the *V amplitude* line ratio, since the relative difference between the gradients of the solid and dashed curves in the weak-field range is considerably smaller for the right diagram of Fig. 2.

The right diagram gives the Stokes V amplitude, $V_{\max}$, normalized to its value when the splitting vanishes, $\Delta\lambda_H(\partial I/\partial\lambda)_{\max}$. This normalization basically expresses the manner in which solar magnetographs are usually calibrated. Neglecting thermodynamic effects in fluxtubes, the curves in the diagram can be seen as representing the ratio between the apparent and true magnetic *fluxes* recorded by the magnetograph. This is the effect that we have called Zeeman saturation in the past (cf. Stenflo, 1976). In addition, the thermodynamic effects reduce the V peak by about the same factor as the Zeeman saturation in the case of the 5250.22 Å line, but these thermodynamic effects are the same in the 5247.06 Å line, so by forming the V amplitude line ratio, the Zeeman saturation effect is isolated, allowing v_H and thus B to be extracted.

The solid and dashed curves in this diagram have the same meaning as for the left diagram. In the asymptotic limit of large Zeeman splitting, $V_{\max}$ approaches $I_c - I_0$ as seen from (1), where I_c is the continuum intensity and I_0 the line center intensity. If we replace $V_{\max}$ by this asymptotic limit, we obtain the dotted curve, a hyperbola, in the diagram (since we divide a constant number by the Zeeman splitting). The 5250.22 Å line has not quite reached this asymptotic limit, whereas the 15648.54 Å line is well inside the asymptotic regime.

We further notice that the solid and dashed curves almost coincide. In particular their gradients are practically identical. This means that the 5250 − 5247 V amplitude line ratio is practically independent of the profile shapes used in the interpretation. We will return to this issue in Sect. 5 below.

When moving from disk center towards the limb the line widths increase, which means that v_H decreases according to (5). Therefore a line that at disk center lies in the completely or partially split regime may move back into the weak-field regime, even if the field strength has not changed when going towards the limb. This is largely the case for the 5250.22 line

and possibly also for the 15648.54 line at the extreme limb. The disappearance of the non-linear effects may give the impression that the fluxtube field strength decreases faster with height than it actually does. We will see examples of this in Sect. 5.

3. Observational material and extracted profile parameters

The FTS observations in the infrared were carried out on May 6–7, 1984, at the McMath telescope of the National Solar Observatory. Stokes I, Q, and V were recorded simultaneously over the spectral range 1.47–1.80 μm, with a spectral resolution (as defined by the maximum path length difference used in the interferometer) of 350,000. Only the small spectral interval covering the 15648.54 Å line will be explored in the present paper. InSb detectors cooled with liquid nitrogen were used.

One scan with the FTS to reach the resolution of 350,000 took about 5.3 min. To enhance the signal-to-noise ratio and to reduce potential systematic line profile distortions several successive scans (between 6 and 10) were made and added for each disk position. The effective time resolution thus varies between 32 and 53 min for the different spectral recordings.

The angular resolution of the recordings is defined by the circular entrance aperture used, which had a diameter corresponding to 5″ on the sun. Eight recordings were made, the disk positions being selected to cover as large a μ (cosine of the heliocentric angle) range as possible. The μ values covered were 1.00 (disk center), 0.76, 0.61, 0.47, 0.43, 0.38, 0.26, and 0.15. The recordings at $\mu = 0.47$ and 0.26 were in sunspots (cf. Fig. 1 above), and will not be analysed here, since the Stokes spectra in sunspots belong to a different category, and therefore cannot be grouped together with plage and network data when exploring general spectral characteristics.

The procedure of selecting magnetic features on the disk was the same as described in Stenflo et al. (1986). In addition, we had to account for the large differential refraction in the earth's atmosphere, since the solar guiders use a visible portion of the spectrum entirely different from the infrared range that the FTS records.

The techniques of piezoelastic modulation to simultaneously record three Stokes parameters with the FTS, heterodyning, polarization calibration, compensation of instrumental polarization, and removal of small residual instrumental polarization are the same as was described in detail in Stenflo et al. (1986) for the recordings in the visible range, and will therefore not be described again here. The level of residual, uncompensated instrumental polarization that had to be removed in the data reduction was on the average 0.03% for Stokes V, 0.09% for Stokes Q.

Figure 3 gives an overview of the signal strength in the 6 non-spot regions observed. V_{max} is the average of the Stokes V amplitudes in the blue and red wings of the 15648.54 Å line. As seen we are dealing with polarization amplitudes in the range 0.3–1.0%. If the true field direction were radial, and the fluxtube field strength and spectral line depth did not vary with μ (no height variation), then V_{max}/μ would be proportional to the magnetic filling factor α. The increase of V_{max}/μ towards the limb shown by the right diagram of Fig. 3 demonstrates that our observations are subject to selection effects, such that the regions closer to the limb generally have a larger filling factor. This effect is difficult to avoid, since signal-to-noise considerations determine a lower limit to the signal strength that we can observe. This lower limit is relatively μ independent (with a moderate increase towards the limb), but when we divide it by μ to transform it to the filling-factor scale of the right diagram of Fig. 3, the increase towards the limb becomes hyperbolic. The average noise level in our recordings, as determined by the standard deviation of the Stokes V and Q fluctuations in the continuous spectrum (where the true signal should be zero) is 0.06%, for both V and Q. The unit used for V and Q throughout the present paper is the intensity of the adjacent continuous spectrum.

The error limits in the μ direction of Fig. 3 and in all the following figures have been estimated by assuming two types of error sources: (1) An error of ±5″, representing the combined effects of aperture size (±2.″5), seeing, and guiding precision. This error is independent of disk position, but as the μ range corresponding to 10″ varies with μ, the error in μ increases rapidly towards the limb. (2) An error in determining the absolute position on the solar disk, which is assumed to increase linearly with limb distance, from zero at the limb to 25″ at disk center. The

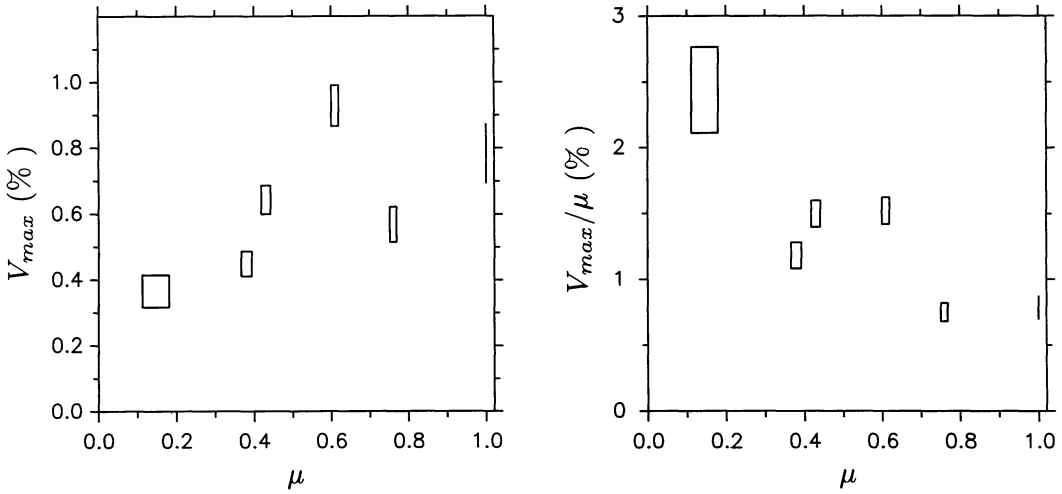

Fig. 3. Polarization signal V_{max}, the average of the Stokes V amplitudes in the blue and red wings of the Fe I λ 15648.54 Å line, with error boxes, for the 6 observed non-spot solar regions

reason for this error is that the disk coordinates of the FTS aperture are measured manually with a ruler, using the limb as a reference. The error naturally increases the further from the limb that we are. This error, however, when translated into a μ scale, is rather minor, so the exact way of estimating it is of no great consequence. It is further assumed that errors (1) and (2) add quadratically. The "anti-McMath" polarization compensator shifts the beam by a large amount, which complicates the precise positioning and is a potential additional error source, but we consider it to be implicitly included in the above treatment.

To explore the center-to-limb behavior of the 15648.54 Å line we have extracted profile parameters defined in the same way as for the corresponding analysis performed in the visible range (Stenflo et al., 1986). In particular we have determined the centers of gravity $\lambda_{V_{b,r}}$ of the upper halves of the blue and red Stokes V peaks as defined in Sect. 2 above, the width v_D of the Stokes I profile in velocity units, also defined in Sect. 2 above, the absolute amplitudes $a_{b,r}$ and areas $A_{b,r}$ of the blue and red V peaks, the wavelength position λ_V of the Stokes V zero crossing, and the center of gravity λ_I of the lower half of the Stokes I profile. In the following section we will describe the center-to-limb variations of combinations of these parameters. The error bars for the parameters have been determined by deriving how the errors (standard deviations in the continuous spectrum) in the Stokes spectra propagate in the defining equations for the respective parameters. The resulting error bars represent the *random* noise in the observations.

4. Directly extracted center-to-limb variations of the Stokes V profile parameters

Our analysis in this section parallels that for the 5250.22 Å line in Stenflo et al. (1986), to make a direct comparison possible.

4.1. Separation of the Stokes V peaks

We saw above in Fig. 2 that at disk center the 15648.54 Å line lies in the strong-field, completely split regime. This means that the separation between the Stokes V peaks, $\lambda_{V_r} - \lambda_{V_b}$, represents the actual Zeeman splitting, and thus gives the field strength directly. In general the completely-split case requires the splitting to be large in comparison with the line width. This may change with μ as the line width increases towards the limb.

Figure 4 shows in the left diagram that the Stokes V peak separation decreases towards the limb, suggesting a corresponding decrease of the field strength (due to an expansion with height of the fluxtubes), provided that the completely-split case applies. The right diagram of Fig. 4 shows the simultaneous rapid increase towards the limb of the Stokes I line width v_D (defined in Sect. 2). When normalizing the Stokes V peak separation in units of the line width by dividing the values in the left by those in the right diagram, the decrease towards the limb of the V peak separation curve becomes even more accentuated.

The line width normalization used in Fig. 5 is the same as was used for Fig. 2. What is plotted is thus $0.5(\lambda_{V_r} - \lambda_{V_b})/(0.425\,\Delta\lambda_I)$, where $\Delta\lambda_I$ is the observed total half width of the Stokes I profile. If the I profile had a Gaussian shape, $0.425\,\Delta\lambda_I$ would be half the separation between the inflexion points of the profile. Comparing

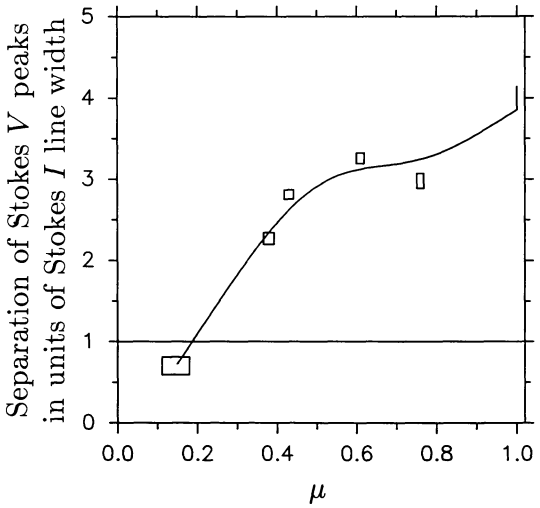

Fig. 5. Center-to-limb variation of $0.5(\lambda_{V_r} - \lambda_{V_b})/(0.425\,\Delta\lambda_I)$ for the 15648.54 Å line, i.e., the observed Stokes V peak separation expressed in units of the line width, defined as for the theoretical curves of Fig. 2

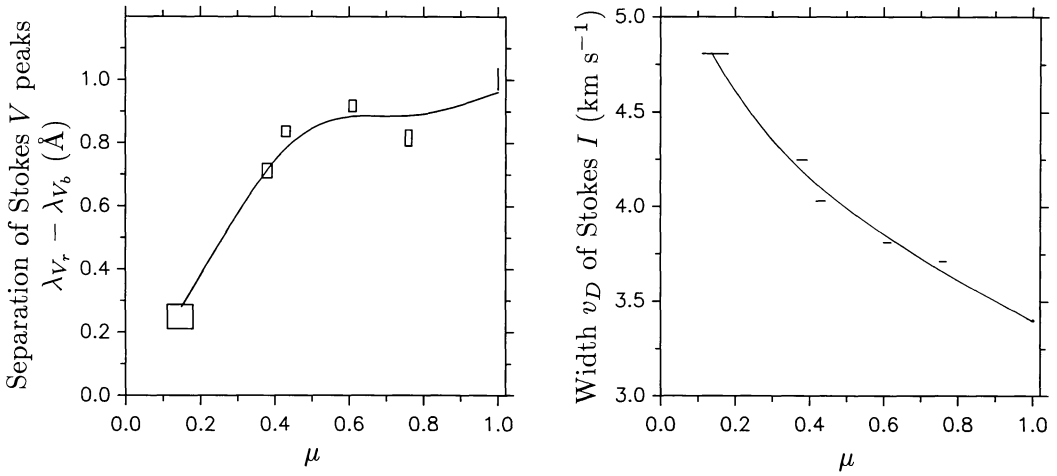

Fig. 4. Left diagram: Center-to-limb variation of the separation between the Stokes V peaks in the red and blue wings of the 15648.54 Å line. The curve is a cubic spline fit. Right diagram: Center-to-limb variation of the width v_D of the corresponding Stokes I profiles, as defined in the text

Fig. 5 with Fig. 2 we see that all the values except the one at $\mu = 0.15$ (about 11″ from the limb) fall within the completely Zeeman-split regime. The circumstance that the value near the limb falls below unity, while Fig. 2 suggests that such values should be forbidden, is most likely due to the difference in thermodynamic properties between fluxtube interior and exterior. As the magnetic filling factor is small the observed Stokes I profile that we have used for the normalization is mainly representative of the non-magnetic surroundings of the fluxtubes, whereas a full comparison with Fig. 2 would require that we normalize with the I profile that originates exclusively inside the fluxtubes (which is not directly observable). If the Stokes I profile of the fluxtube interior is narrower near the limb than the I profile of the fluxtube exterior (e.g. because the Doppler motions perpendicular to the field lines are reduced in the interior, but unconstrained in the exterior), then too low values in Fig. 5 would result, as is the case at $\mu = 0.15$.

Although in the case of the last limb region we are down in the weak-field regime where a straightforward interpretation cannot be made, we can in the μ range $1.0 - 0.3$ directly interpret the V peak separations of Fig. 4 as the actual Zeeman splittings, and conclude that the moderate decline of the values over this μ range really represents a decline of the field strength, corresponding to a fluxtube cross section diverging with height. We will return to this height variation in Sect. 5.

In the case of the 5250.22 Å line (Stenflo et al., 1986), $\lambda_{V_r} - \lambda_{V_b}$ *increased* rapidly towards the limb. The reason for this is that the 5250 line is not fully split, and therefore the V peak separation is dominated by the line width v_D, which increases towards the limb. When the 5250 V peak separation was normalized in terms of the line width, it did decrease towards the limb, as expected. Finally we note that the Stokes I line widths v_D in velocity units are about 20% larger for the 15648.54 Å line as compared with the 5250.22 Å line near disk center, but this difference becomes much smaller near the limb.

4.2. *Stokes V asymmetries and shifts*

Stokes V shifts and asymmetries may be used to diagnose mass motions in the spatially unresolved fluxtubes. We define the relative area and amplitude asymmetries as $(A_b - A_r)/(A_b + A_r)$ and $(a_b - a_r)/(a_b + a_r)$, where $A_{b,r}$ and $a_{b,r}$ are the areas and amplitudes of the blue and red Stokes V peaks. The Stokes V shift relative to Stokes I is defined by $\lambda_V - \lambda_I$, where λ_V is the zero-crossing wavelength of the V profile, and λ_I is the center of gravity of the lower half of the I profile. This Doppler displacement of Stokes V is a measure of the systematic, net mass flows in the fluxtubes, whereas the V asymmetries provide information on the *gradients* of the line-of-sight velocities, and their correlation with magnetic-field gradients.

Our analysis of the 5250.22 Å line showed near disk center an area asymmetry of about +5% and an amplitude asymmetry of about +10%. When approaching the limb the amplitude asymmetry went to zero, while the area asymmetry became negative ($\sim -6\%$).

In the case of the 15648.54 Å line, as shown by Fig. 6, both the area and amplitude asymmetries are close to zero (as is the case for many similarly weak lines in the visible), but they have a clear tendency for *negative* values, which increase in magnitude towards the limb, to typically −4% for the area asymmetry, −8% for the amplitude asymmetry (although the large error boxes do not allow firm conclusions).

The signs of the height gradients of the magnetic and velocity fields inside the fluxtubes are in a simplified theoretical treatment with a quasi-stationary mass flow determined by the sign s_A of the Stokes V asymmetry according to the following condition (cf. Pahlke and Solanki, 1986):

$$s_A \frac{\partial |B|}{\partial h} \frac{\partial v}{\partial h} < 0, \tag{6}$$

where B and v are the line-of-sight components of the magnetic and velocity fields, and h is the height. The sign of v is positive if the motion is *downwards* (positive Doppler shift or redshift). s_A is positive when the blue wing of Stokes V dominates over the red wing. Since for a one-dimensional fluxtube model the magnetic-field gradient can always be expected to be negative (the magnetic field diverges with height), the condition (6) can for such a model be simplified to

$$s_A \frac{\partial v}{\partial h} > 0. \tag{7}$$

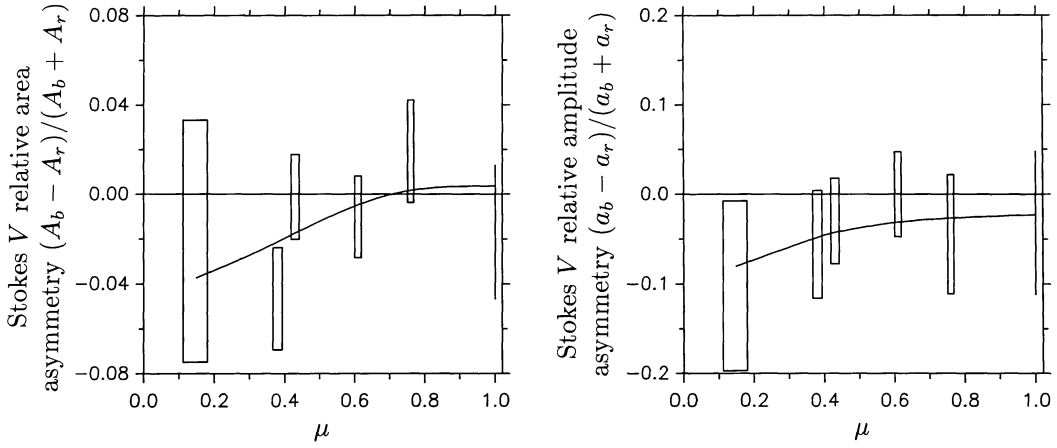

Fig. 6. Center-to-limb variation of the Stokes V relative area (left diagram) and amplitude (right diagram) asymmetries for the 115648.54 Å line. The solid curves are cubic spline fits

Our results for the 15648.54 Å V asymmetry thus indicates that the height gradient of the fluxtube velocity field at the deepest level in the photosphere is opposite in sign as compared with the level where the 5250.22 Å line is formed. This remarkable result again supports the conclusion that we have stressed in all our previous papers on FTS polarimeter data, namely that the observed Stokes V asymmetries, although very likely caused by fluxtube internal mass motions, cannot be explained in terms of quasistationary mass flows. As before we consider fluxtube oscillations to be the most likely explanation of the asymmetries, but a quantitative model interpretation of our data is outside the scope of the present paper. The apparent sign reversal of the Stokes V asymmetries may provide important empirical constraints on any dynamical model of the fluxtubes, but the small asymmetry values and large error bars require that further lines be studied before final conclusions can be drawn.

The results for the Stokes V Doppler shift $\lambda_V - \lambda_I$ relative to the position of the Stokes I profile are plotted in Fig. 7. In contrast to the results for the 5250.22 Å line, which showed values around zero (Stenflo et al., 1986), the V Doppler shift of the 15648.54 Å line is as high as about $1\,\mathrm{km\,s^{-1}}$ near disk center, decreasing to small values ($\lesssim 0.4\,\mathrm{km\,s^{-1}}$) near the limb. Although this disk-center value is high in comparison with the results from our previous FTS data in the visible, it is smaller by about a factor of two than the value given by Harvey (1977) for the same spectral line. The earlier measurements are inferior to the present work and were likely to have been affected by systematic scanning errors.

The Doppler shifts given by Fig. 7 however do not necessarily represent actual motions in the fluxtubes, since the reference wavelength λ_I of the Stokes I profile (which is representative of the fluxtube surroundings) is blueshifted due to the brightness-velocity correlation in the solar granulation. At visible wavelengths there exist empirical and theoretical determinations of this granulation-induced blueshift, which we could use to establish a corrected zero-line reference level for our Stokes V center-to-limb data (Stenflo et al., 1986). In the infrared, however, no such determinations exist, so no corrected zero level can be introduced in Fig. 7.

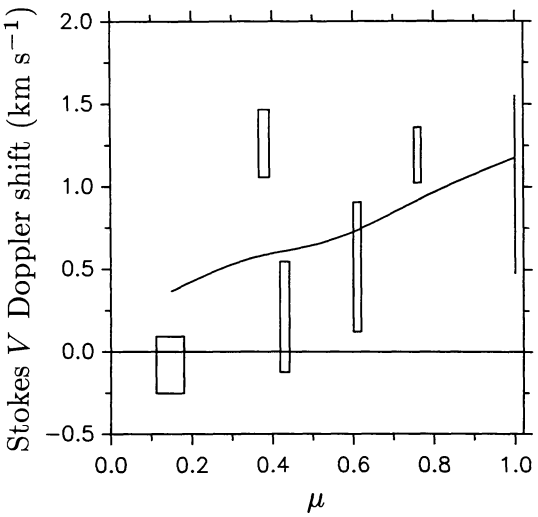

Fig. 7. Center-to-limb variation of the Doppler shift of the Stokes V zero-crossing wavelength relative to the center of gravity of the lower half of the Stokes I profile, expressed in velocity units, for the 15648.54 Å line. The solid curve is a cubic spline fit

Nevertheless we can get a general idea of the magnitude of the zero-line correction through the following considerations. The relatively weak 15648.54 Å line, being located where the opacity minimum in the solar spectrum occurs, is formed near the bottom of the photosphere, much below the upper photospheric levels where the Fe I lines in the visible are formed. As the intensity of the solar granulation increases with depth, it is natural to expect the granulation-induced blueshift to be more pronounced in the infrared. This expectation is supported by the results for Fe II lines in the visible by Dravins et al. (1986), who find a mean granulation-induced blueshift at disk center for these lines of about $0.8\,\mathrm{km\,s^{-1}}$ (with a scatter of about $0.4\,\mathrm{km\,s^{-1}}$). As the 15648.54 Å line is expected to be formed even deeper than the visible Fe II lines, the granulation-induced blueshift should be quite large also for this line.

Balthasar (1985) has determined the granulation-induced blueshift at disk center as a function of optical depth τ in the continuum at 5000 Å, for $-1 < \log\tau < -5$. If we make a linear extrapolation of his results to $\log\tau = 0$, which we estimate to be the typical depth of formation of our IR line, we obtain a blueshift of 900–$1000\,\mathrm{m\,s^{-1}}$, comparable to our measured apparent redshift.

On the basis of these arguments we consider it likely that the apparent Stokes V Doppler shifts of Fig. 7 would not significantly differ from zero if a proper zero-line correction due to the granulation-induced blue shift of Stokes I had been introduced. As such a correction is presently not possible, we have to leave Fig. 7 as being inconclusive concerning systematic fluxtube mass motions.

4.3. *Stokes Q behavior*

For a completely split Zeeman triplet the Stokes Q $\sigma - \pi$ asymmetry, defined by $(a_\sigma - a_\pi)/(a_\sigma + a_\pi)$, where a_σ is the sum of the Q amplitudes of the two σ components and a_π is the amplitude of the π component, should be zero in the case of weak lines with little saturation, like the 15648.54 Å line. Our results show that the observed Q $\sigma - \pi$ asymmetry is indeed zero when we are closer to disk center than $\mu \approx 0.6$, with a slight tendency to increase somewhat towards the limb (to about 0.2 at $\mu = 0.38$; the last limb position, at $\mu = 0.15$, was too noisy in Q to be analysed). These results differ greatly from those obtained for the 5250.22 Å line, which showed a much larger asymmetry, increasing to about 0.6 near the limb (Stenflo et al., 1986). The difference can be understood in terms of the incomplete Zeeman splitting of the 5250.22 Å line and the difference in line strength (i.e. saturation) between the two profiles.

The Stokes Q/V ratio on the other hand shows a behaviour very similar to that of the lines in the 5246–5252 Å range. The Q/V ratio is defined as $Q_{\max}\mu/[V_{\max}(1-\mu^2)]$, where $Q_{\max}$ and $V_{\max}$ represent the average of the Q and V amplitudes of the two σ components. The μ factors have been introduced to make the ratio independent of μ in the case that the field is constant and directed along the solar radius. As explained in Stenflo et al. (1986), the Q/V ratio is a function of both the direction and intrinsic strength of the field. For more complete diagnostics of the field direction, observations of the missing Stokes parameter, U, would be needed. Since no such data are available yet, we

refrain from trying to extract information on the field direction from the Q/V ratio in the present paper.

5. Field strength height variation in the fluxtubes

With Eq. (1) we have shown how the Stokes V profile may be expressed as the difference between the Zeeman-shifted Stokes I profiles. More explicitly for the fluxtube case we have

$$V = \tfrac{1}{2}\alpha[I_V(\lambda + \Delta\lambda_H) - I_V(\lambda - \Delta\lambda_H)], \quad (8)$$

where α is the magnetic filling factor. By writing I_V instead of I we emphasize that I_V is not the observed I, but the Stokes I that originates exclusively inside the spatially unresolved fluxtubes (and therefore cannot be directly observed). Normally I_V and I differ greatly from each other due to the different thermodynamical conditions between fluxtube interior and exterior (cf. Solanki and Stenflo, 1984). The most important difference is in the depth of the lines, to a lesser extent in their shapes. Incorrect estimates of the I_V line depth will lead to errors in the filling factor α.

To obtain a direct determination of the magnetic field strength from the Stokes V profiles of any line, regardless of whether the Zeeman splitting is complete or not, we have applied the model described by Eq. (8) instead of at this stage of the analysis entering into extensive radiative-transfer calculations. The model is characterized by the two free parameters α and $\Delta\lambda_H$, and by the means of choosing I_V. In our crude application we have replaced the unobservable I_V by the observed Stokes I. Although this procedure gives us unreliable or even useless values of the filling factor α, the determination of the Zeeman splitting $\Delta\lambda_H$ is almost unaffected.

An iterative least squares technique has been used to determine the values of the two free parameters α and $\Delta\lambda_H$ that provide the optimum fit to the observed Stokes V profile. All the wavelength points in the profile contribute to the fit with equal weight. The value obtained for $\Delta\lambda_H$ gives the fluxtube field strength B. The value of the filling factor is however not used further, since it is too strongly influenced by the unknown thermodynamic fluxtube effects.

Figure 8 shows the results of this analysis as applied to the V and I profiles observed in the 15648.54 Å line at the 6 selected disk positions. The left diagram gives the extracted field strength B vs. μ. The fluxtube field strength decreases from 1.49 kG at disk center to 1.09 kG at $\mu = 0.38$, which agrees well with the field strength of between 1200 and 1700 G given by Harvey (1977) for this line near disk center. The very low value of 0.11 kG at $\mu = 0.15$ should be judged with great caution, since a determination so close (11″) from the limb is bound to be very uncertain.

Since the Zeeman splitting of the 15648.54 Å line is complete for $\mu \gtrsim 0.3$ as we have seen from Sect. 4.1 and Fig. 5, we could for this μ range have used the separation between the Stokes V peaks as given by Fig. 4 directly to extract the field strength B. In this case the two approaches are in principle equivalent (the least squares technique gives smaller formal error bars, since more wavelength points are used, and the procedure of deriving standard deviations is different). It is in the incomplete splitting regime, which applies to the 5250 – 5247 Å lines that will be analysed below, where the V peak separation cannot be used directly, but where our modelling with the least squares fitting is really needed.

For a cylindrical fluxtube with radius r we can express the flux Φ from the nearly vertical field of strength B as $\Phi = \pi r^2 B$. Since Φ is expected to be height independent for an aperture of 5″ diameter, the fluxtube radius

$$r \sim 1/\sqrt{B}\,. \quad (9)$$

The height of formation decreases with μ, i.e., increases with $1 - \mu$. Therefore $1 - \mu$ can be regarded as a height scale with an arbitrary zero level. We have accordingly converted the B vs. μ data of the left diagram of Fig. 8 into the right diagram, giving $1 - \mu$ vs. $1/\sqrt{B}$. Since the $\mu = 0.15$ point is quite uncertain, it has been omitted in this plot. Qualitatively we can interpret this diagram as giving the height vs. fluxtube radius. It gives us an immediate

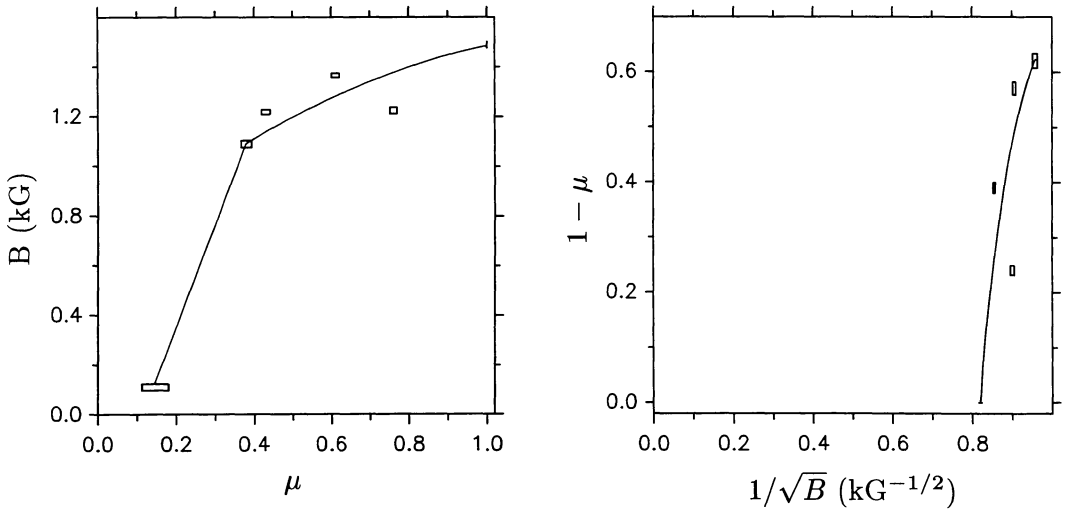

Fig. 8. Left diagram: Field strength B vs. μ as derived from the observed Stokes V and I profiles of the 15648.54 Å line, using (8) and a linearized least squares fitting technique as described in the text. Right diagram: The data of the left diagram transformed to a plot of $1 - \mu$ vs. $1/\sqrt{B}$, giving according to (9) a direct impression of how the fluxtube radius varies with height

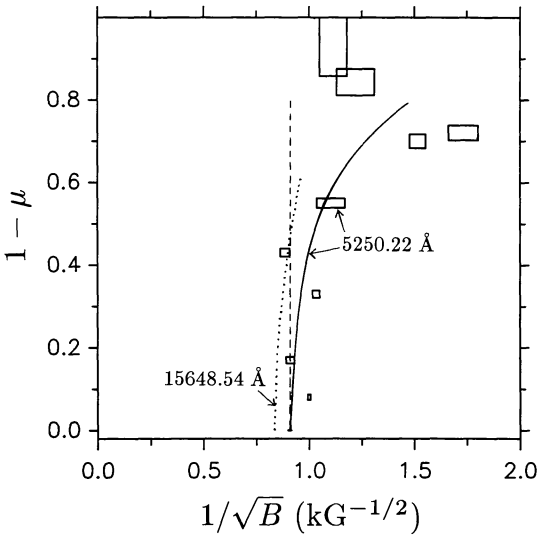

Fig. 9. Height variation of the fluxtube radius, as represented by $1-\mu$ vs. $1/\sqrt{B}$. The error boxes have been derived from the observed Stokes V and I profiles of the 5250.22 Å line using (8) and a linearized least squares fitting technique. The solid curve represents our estimated smooth fit to the data, and is used as input to the line-ratio calculations of Fig. 10. The dotted curve shows the corresponding results of Fig. 8 for the 15648.54 Å line. The vertical dashed line represents a height-independent field that is used as input to the line-ratio calculations of Fig. 10

impression of how the fluxtube cross section increases with height, or of the shape of the fluxtube boundary.

The same procedure of using (8) to model the Stokes V profile has also been applied to our Stokes V and I data for the 5250.22 Å line, for which such modelling is really needed since the splitting is incomplete. The results are given by the error boxes in Fig. 9, through which we have drawn a smooth curve to indicate the estimated general trend of the data. The scatter of the computed field strengths is much larger as compared with the results for the 15648.54 Å line, which is expected since the splitting is much smaller and incomplete. In this case errors in the model assumption that the observed Stokes I equals I_V will have a greater effect on the computations.

For comparison we have also in Fig. 9 plotted (dotted curve) the average relation obtained in Fig. 8 for the infrared 15648.54 Å line. The infrared line gives systematically somewhat larger field strengths, i.e., smaller fluxtube radii. This is expected, since this line is formed deeper in the atmosphere. The height gradient of the magnetic field can thus be evaluated in two ways: (1) Via the observed center-to-limb variation in each line. (2) Via the average difference in the derived B between the two lines, divided by the difference in height of formation. Figure 9 indicates that these two methods will give the same values for the height gradient provided that the difference in height of formation at disk center between the 5250.22 and 15648.54 Å lines is about the same as the difference in height of formation for the 15648.54 Å line at disk center ($\mu = 1.0$) and at $\mu \approx 0.5$ (approximately where the dotted curve crosses the vertical dashed line).

Information on the height gradient of the magnetic field is also contained in the 5250 − 5247 V amplitude and peak separation line ratios. To explore the relation between the various diagnostic approaches we have transformed the solid and dashed curves in Fig. 9 to line ratio vs. μ, using Eq. (8) to model the V profile. In the case of the 5247.06 Å line, which has an anomalous splitting pattern, (8) has been generalized to describe the weighted superposition of all the σ components with their various Zeeman shifts. However, calculations using an effective Landé factor g_{eff} to characterize the full splitting pattern give practically identical results. The results of these computations are displayed in Fig. 10 together with the corresponding observational data, taken from Stenflo et al. (1986). The reason for also showing the dashed line of Fig. 9, which corresponds to zero height gradient of B, is to isolate the line-width effect from the magnetic-field effect in the center-to-limb variation of the line ratios (see below).

The practical procedure of calculating the line ratio from the given B values has been the following: Using for I_V in (8) the 5247.06 Stokes I profile as observed at $\mu = 1.00$, we have calculated the model Stokes V profiles resulting from the Zeeman splitting patterns of the 5250.22 and 5247.06 Å lines, respectively, for a range of field strength values B. As the filling factor disappears when forming the line ratio, an arbitrary value can be used. The 5247.06 I profile is used rather than the 5250.22 profile even to represent I_V of the 5250 line, since the 5247 line has a smaller Zeeman splitting. Ideally the I_V profile in (8) should be the *unsplit* I profile that originates exclusively in the fluxtubes, i.e., the profile that would occur if the Landé factor were zero.

Next we have used the model Stokes V profiles to derive the corresponding V amplitude and peak separation line ratios, defined exactly as when they were derived from the observed Stokes V profiles, as functions of the field strength B. We have to recall, however, that these relations only apply to the disk center, since a disk center I profile was used as input in the calculations. At other disk positions we have to take the μ-dependent width of the Stokes I profile into account.

We have seen from Sect. 2 and Fig. 2 above that the nonlinear magnetic-field effects on the Stokes V profile depend rather uniquely on v_H, the *ratio* between the Zeeman splitting and the line width, not on the Zeeman splitting or the field strength alone. This splitting – width ratio is proportional to B/v_D, where v_D is the I line width in velocity units. Thus if at disk center a 1 kG field gives a certain value of the line ratio, a stronger field is required to produce the same line ratio at other disk positions if the line width increases towards the limb. Conversely if the fluxtube field strength does not vary with μ, variations in the line ratios will be induced by the line-width effect alone. Accordingly the dashed lines in Fig. 10 would be horizontal if there were no center-to-limb variation of v_D.

To obtain the model values of the line ratios for arbitrary μ values for a given input B value we have to divide B by the v_D value for that μ position, and read off the relations derived for the disk center at the corresponding B/v_D value there. A smooth function fitting the observed v_D vs. μ for the 5247 line was used to represent the line widths of the non-split 5250 and 5247 I_V profiles for arbitrary μ values.

In this way the solid and dashed curves of Fig. 10 have been produced using the corresponding curves of Fig. 9 as input to the calculations. The difference between the dashed curve and a horizontal line that coincides with the dashed curve at $\mu = 1.0$ is exclusively due to the effect of the increase in the non-magnetic line width when approaching the limb. The difference between the solid and dashed curves on the other hand is exclusively due to the height variation of the magnetic field B (cf. the difference between the solid and dashed curves in Fig. 9).

The agreement between the solid curve and the observed line ratio is quite good in the case of the V amplitude line ratio

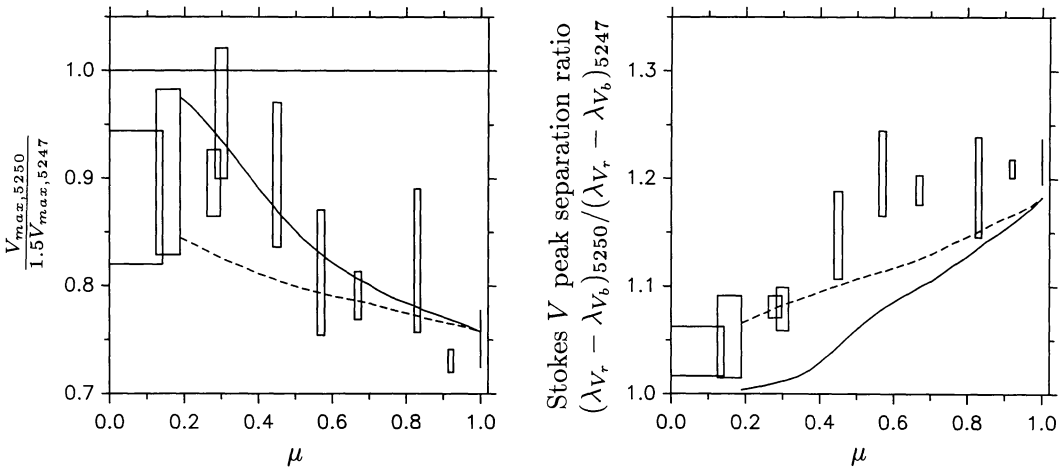

Fig. 10. Observed and computed 5250 – 5247 line ratios. The left diagram gives the V amplitude line ratio, the right diagram the V peak separation line ratio. The observational data have been taken from Stenflo et al. (1986). The solid and dashed theoretical curves have been computed using the solid and dashed curves of Fig. 9 as input

(left diagram of Fig. 10), indicating that the procedure used to choose the unobservable I_V profile for the model Eq. (8) has been satisfactory. In the case of the V peak separation line ratio on the other hand (right diagram) the agreement between the model and the data is poor. If we modify the model by changing the input B values and/or the assumption for the I_V data used, such that a better model fit to the V peak separation data is obtained, then the fit to the V amplitude line ratio gets correspondingly worse. The model of Eq. (8) is unable to *simultaneously* reproduce the two types of observed line ratios.

The failure of the model (8) has been revealed by the difference in the fits to the observed V amplitude and peak separation line ratios, demonstrating that these two types of line ratios are not diagnostically equivalent. The superposition of Zeeman-shifted I profiles used in (8) is only valid for homogeneous longitudinal magnetic fields without any velocity gradients. We have searched for the cause of the poor fit to the V peak separation line ratio by comparing the model V profiles with the corresponding observed ones. The source of the problem appears to be the large asymmetries in the observed Stokes V profiles, which cannot be reproduced by this type of model. The main difference between the model and the observed V profile seems to be that the red peak of the observed V profile is differentially suppressed on the side facing the line center, as if there were selectively enhanced absorption in this portion of the line profile. This effect causes the center of gravity of the red V peak to be pushed further towards the red, making the observed V peak separation larger than can be reproduced by our model, which only produces V profiles anti-symmetric with respect to the zero-crossing wavelength.

Apparently the V amplitude line ratio is much less affected by this effect of the V asymmetry, since there is consistency between the B height gradient deduced in Fig. 9 and the line ratio of Fig. 10. Already in Sect. 2 in the discussion of Fig. 2 we noticed that the Stokes V peak separation was considerably more dependent on the *shape* of the I profile used as compared with the V amplitude, which supports our present conclusions. We thus have to be careful when using the V peak separation for diagnostic purposes in the case that the Zeeman splitting is not complete. We notice however in Fig. 10 that both line ratios give results that are fairly consistent with each other at disk center, and that the discrepancies really develop when moving away from the disk center.

If the Stokes V asymmetries are to be modelled, we have to make radiative-transfer calculations using a dynamic fluxtube model with mass motions. As however no stationary flows can explain the asymmetries *and* zero-crossing shifts simultaneously (Stenflo, 1984; Pahlke and Solanki, 1986), and as the nature of the mass motions is not well understood (likely candidate processes: fluxtube oscillations and waves), time is not yet ripe for a full theoretical treatment of this problem. In any case we need to be aware of the effects that the asymmetries may have on diagnostic parameters used, like in the present case the V peak separation line ratio.

As noted above, the I_V profile originating in the fluxtube is generally different from the observed I profile. In the case of a fully split line and a homogeneous magnetic field this difference can be made directly visible, since the shapes of the two σ components are simply given by the shapes of the blue and red Stokes V peaks. In Fig. 11 we compare the Stokes V profiles observed at $\mu = 1.00$ and 0.61 (solid curves) with the corresponding model curves (dashed) obtained using (8) and the linearized least squares fitting procedure that was used to calculate the field strengths plotted in Figs. 8 and 9. The wavelength scale has been transformed to field-strength units (kG), using the Landé factor of 3.0 for the 15648.54 Å line. This allows us to read off the field strength directly from the observed Zeeman splitting in the diagrams.

We notice that the observed Stokes V peaks are systematically much broader than the corresponding model V peaks, based on using the observed Stokes I to represent the σ components. Such broadening has been noticed previously (e.g. Harvey et al., 1972). It could have two possible causes: (1) The magnetic field is not single-valued in the fluxtubes, but there is a distribution of field strengths, which gives rise to a Zeeman broadening of the σ components. (2) There is more Doppler broadening (thermal and/or non-thermal) inside the fluxtubes than outside. With the 15648.54 Å line alone we cannot distinguish between these two alternatives.

The Doppler and Zeeman broadening effects can be separated by comparing the behavior of lines with different Landé factors. Thus for most lines at visible wavelengths the Zeeman broadening

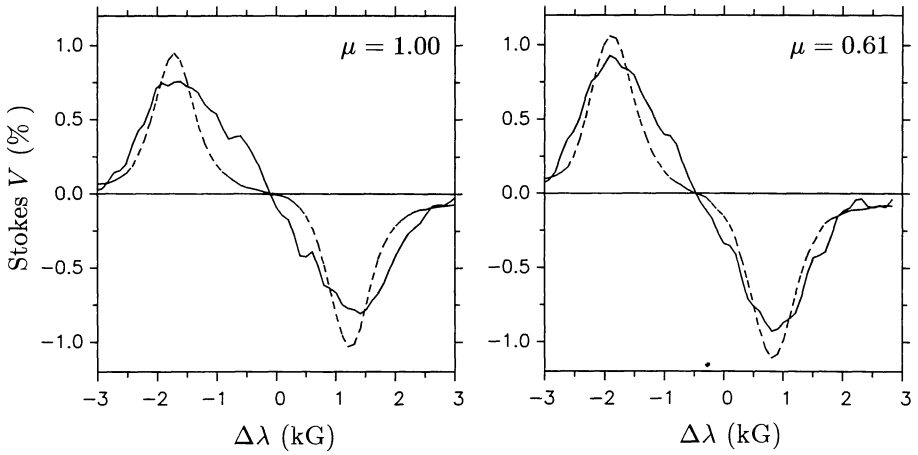

Fig. 11. Comparison between observed (solid curves) and computed (dashed curves) Stokes V profiles at $\mu = 1.00$ and 0.61. The relative wavelength scale has been transformed to kG units (based on a Landé factor of 3.0) to allow the field strengths to be read off directly from the observed Zeeman splitting. The zero point of the $\Delta\lambda$ scale refers to the nominal wavelength of 15648.6 Å, *not* to the V zero crossing wavelength. The dashed curves represent the model fits that were used to obtain Fig. 8. Due to additional Zeeman and/or Doppler broadening inside the fluxtubes the observed σ components are wider than the computed ones

is insignificant, and the widths of the σ components can be explained in terms of Doppler broadening alone. It is only by using large-splitting Zeeman triplets like the 15648.54 Å line that we may be able to diagnose the *distribution* of field strengths in the fluxtube interiors.

6. Concluding remarks

The infrared region of the spectrum around 1.5 μm introduces a new dimension to the study of fluxtube diagnostics. Due to the wavelength dependence of the Zeeman splitting we can find infrared lines that are completely split in the fluxtubes, whereas this is not possible in the visible. As the continuum opacity has a minimum around 1.6 μm, we can reach down to atmospheric layers that cannot be diagnosed at other wavelengths.

In the present paper we have explored the diagnostic possibilities in the infrared using the observed center-to-limb variations of the Stokes profiles of the 15648.54 Å line. In particular we have tried to relate the methods for magnetic-field diagnostics in the infrared and visible ranges to each other and to provide a unified overview of the connections, merits, and limitations of using spectral lines with small, partial, or complete Zeeman splittings. The line-ratio technique, for instance, was devised to remove model dependence when determining field strengths using lines that are only partially split. The results for the Stokes V *amplitude* line ratio, which is the type of line ratio that has been exploited in the past, are consistent with the complete splitting results for the infrared line. The V peak separation line ratio on the other hand seems to be affected by the large asymmetries in the Stokes V profiles due to the gradients of the Doppler velocities in the fluxtubes. These Stokes V asymmetries appear to be of opposite sign (red V peak larger than the blue one) in the infrared line as compared with previous results obtained at visible wavelengths. This indicates that the corresponding time-averaged gradients in the Doppler velocities change sign when going down to the bottom of the fluxtube photosphere.

We have further obtained determinations of the fluxtube field strength as a function of center-to-limb distance, and have converted these results into a diagram that gives a qualitative picture of the height increase of the fluxtube radius. Comparison between the widths of the observed Stokes V σ components with the widths of the corresponding I profiles indicates significant broadening and illustrates that it may be possible to extract information on the internal *distribution* of field strengths in the fluxtubes by comparing the shapes of the σ components of lines of different but large Zeeman splittings.

The aim of the present paper has been to explore and clarify various new possibilities for the diagnostics of the spatially unresolved magnetic fluxtubes, to provide a foundation for building empirical fluxtube models. To exploit these possibilities, and in particular to establish a geometrical height scale for the various parameters, one needs numerical, self-consistent models of the fluxtube atmospheres, from which one can via radiative transfer calculate the emergent Stokes profiles to be compared with the observed ones. We also need to analyse more lines in the infrared and make FTS recordings in more solar regions with different magnetic filling factors, to obtain a more complete observational data base to be used for the construction of empirical fluxtube models.

Acknowledgements. We are grateful to R. Hubbard for assistance in the operation of the FTS system, and to G. Ladd for carrying out the Fourier transforms and converting the data to a usable format. The work of one of us (S.K.S.) was supported by grants No. 2.814-0.83 and 2.666-0.85 from the Swiss National Science Foundation.

References

Balthasar, H.: 1985, *Solar Phys.* **99**, 31
Brault, J.W.: 1978, *Osserv. Mem. Astrofis. Arcetri* **106**, 33
Dravins, D., Larsson, B., Nordlund, Å.: 1986, *Astron. Astrophys.* **158**, 83
Goldberg, L., Mohler, O.C., McMath, R.R.: 1949, *Astrophys. J.* **109**, 28
Harvey, J.W.: 1977, in E.A. Müller (ed.), *Highlights of Astronomy* **4**, 223
Harvey, J., Hall, D.: 1975, *Bull. Am. Astron. Soc.* **7**, 459
Harvey, J., Livingston, W., Slaughter, C.: 1972, *Line Formation* in the Presence of Magnetic Fields, High Altitude Observatory, Boulder, p. 227
Litzén, U.: 1976, *Physica Scripta* **14**, 165
Pahlke, K.D., Solanki, S.K.: 1986, *Mitt. Astron. Gesellschaft* **65**, 162

Solanki, S.K., Stenflo, J.O.: 1984, *Astron. Astrophys.* **140**, 185
Solanki, S.K., Stenflo, J.O.: 1985, *Astron. Astrophys.* **148**, 123
Stenflo, J.O.: 1973, *Solar Phys.* **32**, 41
Stenflo, J.O.: 1975, *Solar Phys.* **42**, 79
Stenflo, J.O.: 1976, in V. Bumba, J. Kleczek (eds.), *IAU Symp.* **71**, 69
Stenflo, J.O.: 1984, *Adv. Space Res.* **4**, 5
Stenflo, J.O.: 1985, *Solar Phys.* **100**, 189
Stenflo, J.O., Harvey, J.W.: 1985, *Solar Phys.* **95**, 99
Stenflo, J.O., Harvey, J.W., Brault, J.W., Solanki, S.K.: 1984, *Astron. Astrophys.* **131**, 333
Stenflo, J.O., Lindegren, L.: 1977, *Astron. Astrophys.* **59**, 367
Stenflo, J.O., Solanki, S.K., Harvey, J.W.: 1986, *Astron. Astrophys.* (in press)